

# X-ray Signatures of an Ionized Reprocessor in the Seyfert galaxy Ton S 180

T.J.Turner<sup>1,2</sup>, I.M. George<sup>1,2</sup>, K. Nandra<sup>1,3</sup>

## ABSTRACT

We discuss the hard X-ray properties of the Seyfert galaxy Ton S 180, based upon the analysis of *ASCA* data. We find the X-ray flux varied by a factor  $\sim 2$  on a time scale of a few thousand seconds. The source showed significantly higher amplitude of variability in the 0.5–2 keV band than in the 2–10 keV band. The continuum is adequately parameterized as a  $\Gamma \sim 2.5$  power-law across the 0.6–10 keV band. We confirm the recent discovery of an emission line of high equivalent width, due to Fe K-shell emission from highly-ionized material. These *ASCA* data show the Fe line profile to be broad and asymmetric and tentatively suggest it is stronger during the X-ray flares, consistent with an origin from the inner parts of an accretion disk. The X-ray spectrum is complex below 2 keV, possibly due to emission from a blend of soft X-ray lines, which would support the existence of an ionized reprocessor, most likely due to a relatively high accretion rate in this source.

*Subject headings:* galaxies:active – galaxies:nuclei – X-rays: galaxies – galaxies: individual(Ton S 180)

## 1. Introduction

Ton S 180 (PHL 912) is the brightest Active Galactic Nucleus (AGN) detected by the Extreme Ultraviolet Explorer (*EUVE*; Bowyer et al. 1996) as it is a strong emitter in the ultraviolet regime and also has a low Galactic column density along the line-of-sight ( $N_H = 1.52 \times 10^{20} \text{cm}^{-2}$ ; Stark et al. 1992). This source has FWHM  $H\alpha$  and  $H\beta \sim 900 \text{km s}^{-1}$

---

<sup>1</sup>Laboratory for High Energy Astrophysics, Code 660, NASA/Goddard Space Flight Center, Greenbelt, MD 20771

<sup>2</sup>Universities Space Research Association

<sup>3</sup>NAS/NRC Research Associate

and a redshift  $z=0.06198$  (Wisotzki et al. 1995). The absolute magnitude is  $M_B = -23.1$ , on the borderline often used to (arbitrarily) distinguish Seyfert galaxies and quasars.

A terminology has developed which names a subclass of Seyfert 1 galaxies as narrow-line Seyfert 1 galaxies (NLSy1). This name is somewhat confusing: objects classed as NLSy1 are loosely defined as having the narrowest optical permitted lines in the distribution covered by Seyfert 1 galaxies. Typically the widths of the broad components of  $H\alpha$  and  $H\beta$  are only slightly broader than the forbidden lines,  $\text{FWHM } H\beta < 2000 \text{ km/s}$  (although some authors consider only sources with FWHM of the Balmer lines  $< 1500 \text{ km/s}$  to be NLSy1) and  $[\text{OIII}]/H\beta < 3$ , to distinguish them from Seyfert 2 galaxies. Strong FeII emission is often present in sources with the narrowest permitted lines. An alternative, less common name for these objects is I ZW 1 objects, which is a well-studied example of this type (Halpern & Oke 1987). However, the emerging consensus of opinion seems to be that there is a distribution of widths of the permitted lines, and other properties, and so the definition of a subclass can be considered somewhat arbitrary (Lawrence et al. 1997). Nevertheless, the properties of Ton S 180 have lead it to be commonly referred to as a NLSy1.

The strong anti-correlation between soft X-ray slope and FWHM  $H\beta$  (Boller et al. 1996) is of interest and may explain why the list of bright AGN detected by *EUVE* is dominated by sources with relatively narrow permitted lines. Brandt et al. (1997) showed the correlation also exists between hard X-ray spectrum (2–10 keV slope) and FWHM  $H\beta$ . It has been speculated that these effects may be due to a difference in a fundamental parameter such as the accretion rate (e.g. Pounds et al 1995). Large amplitude and rapid X-ray variability also appears most common in objects with narrow permitted lines, and could extend into the extreme ultraviolet regime. For example, Ton S 180 has been reported to show a “doubling time” of 12 hours in an *EUVE* observation (Hwang & Bowyer 1997).

The *ROSAT* PSPC made 15 pointed observations of Ton S 180, and the source was also detected in PSPC survey data taken during 1990 Dec 16-18 (Fink et al. 1997). The source showed flux variability up to a factor of  $\sim 2$  on timescales of hours to years, including some flare-type outbursts. Fink et al. find a complex spectrum which can be parameterized by a power-law  $\Gamma = 3.1_{-0.05}^{+0.05}$  plus a black-body of temperature  $kT = 15.7_{-2.5}^{+2.5} \text{ eV}$ , dominating below 0.3 keV, both absorbed by a column consistent with the Galactic line-of-sight value. However, *EUVE* yields a flux density  $\nu F_\nu = 3.9 \times 10^{-11} \text{ erg cm}^{-2} \text{ s}^{-1}$  at 0.14 keV (Vennes et al. 1995), a factor of five lower than the extrapolation of the model to the PSPC data (Fink et al. 1997). The PSPC data show that the spectrum of the source was consistent with being constant across many of the observations, although a flattening of the power-law component was noted between the observations on 1992 Dec 18 and 1993 Jan 10, when the source was at approximately the same flux-state.

Comastri et al. (1998) confirmed the narrow widths of the optical permitted lines using a spectrum taken at the ESO 1.52m telescope and presented the results along with the *BeppoSAX* observation of Ton S 180 taken on 1996 Dec 3. The effective exposure time was  $\sim 25$ ks with the Medium Energy Concentrator Spectrometer (MECS) which covers 1.3 – 10 keV, and  $\sim 12$  ks with the Low Energy Concentrator Spectrometer (LECS) which covers 0.1 – 10 keV. The *BeppoSAX* paper reported the first spectrum of Ton S 180 above 2 keV, which could be parameterized adequately using a double power-law model with  $\Gamma \sim 2.3$  above 2 keV, and  $\Gamma \sim 2.7$  below 2 keV. Comastri et al. (1998) found significant iron  $K\alpha$  emission at a rest-energy  $\sim 7$  keV, suggesting the line has an origin in ionized material.

Here we present the results of the *ASCA* observation of Ton S 180, which comprises the only other hard X-ray information available to date. In §3 we discuss the time variability of the source. §4 details the mean X-ray spectrum and in §5 we present a tentative result on spectral variability in the source.

## 2. ASCA Observations and Data Reduction

*ASCA* (Makishima et al. 1996) has four co-aligned X-ray telescopes with two solid-state imaging spectrometers (SISs; Burke et al. 1994) and two gas imaging spectrometers (GISs; Ohashi et al. 1996) in the focal plane, yielding effective bandpasses  $\sim 0.4$ –10 keV and  $\sim 0.8$ –10 keV respectively. Ton S 180 was observed by *ASCA* on 1996 July 10 – 11. The data were reduced in the same way as the Seyfert galaxies presented in Nandra et al. 1997a (N97a) and Turner et al. 1997. For details of the data reduction method see N97a. Data screening yielded effective exposure times of  $\sim 44$  ks in the SIS and  $\sim 49$  ks in the GIS instruments. SIS response matrices were created using *SISRMG v1.1*. In this paper, all energy ranges are given in the observers frame, unless otherwise noted.

## 3. Time Variability

The flux in the 0.5 – 2 keV band was  $1.1 \times 10^{-11}$  erg cm $^{-2}$ s $^{-1}$  during the *ASCA* observation, similar to some of the flux states observed by *ROSAT* (Fink et al. 1997). The 2 – 10 keV flux was  $6.0 \times 10^{-12}$  erg cm $^{-2}$ s $^{-1}$  inferring a luminosity of  $\sim 10^{44}$  erg s $^{-1}$  (assuming  $H_0 = 50$  km s $^{-1}$  Mpc $^{-1}$ ,  $q_0 = 0.5$ ). These *ASCA* fluxes are determined assuming a spectral model consisting of a power-law plus Gaussian “hump”, as detailed in §4.1. We note that any model providing a good fit to the data will yield a flux which is accurate to  $\sim 10\%$ . For comparison, the *BeppoSAX* observation found the source to have a 2 – 10 keV flux

$4.2 \times 10^{-12} \text{erg cm}^{-2} \text{s}^{-1}$  (Comastri et al. 1998).

Fig. 1 shows soft (0.5 – 2 keV) and hard (2 – 10 keV) light curves, constructed using 128 s bins, along with their ratio. Ton S 180 shows variations in flux by a factor  $\sim 2$ , with the most significant variations evident in the 0.5 – 2 keV band. We investigated the “excess-variance” ( $\sigma_{rms}^2$ ) for the light curves. This quantity is a measure of the amplitudes of deviations from the mean flux, in excess of those expected from statistical scatter within the light curve (for a detailed definition of this quantity see N97a). The light curve taken over the full 0.5–10 keV band shows  $\sigma_{rms}^2(0.5 - 10 \text{keV}) = 0.026 \pm 0.003$ . In Fig. 2a we show  $\sigma_{rms}^2(0.5 - 10 \text{keV})$  versus luminosity for Ton S 180 compared to the Seyfert 1 sample of N97a; three sources for which it could be measured in the Seyfert 2 sample (Turner et al. 1997) and some recent measurements for NGC 3783 and NGC 3227 (George et al. 1998a, 1998b). Ton S 180 clearly shows larger  $\sigma_{rms}^2(0.5 - 10 \text{keV})$  than expected for a typical Seyfert 1 galaxy of that luminosity.

Next we examined  $\sigma_{rms}^2(2 - 10 \text{keV})$  i.e. that measured in the hard band alone, and the results are shown in Fig. 2b. In this band, Ton S 180 has  $\sigma_{rms}^2(2 - 10 \text{keV}) = 0.013 \pm 0.005$  which is not so significantly separated from the rest of the distribution, compared to the “full-band” result (Fig. 2a). We also note that  $\sigma_{rms}^2$  is significantly greater (at 99% confidence) in the 0.5 – 2 keV band than in the 2 – 10 keV band, with  $\sigma_{rms}^2(0.5 - 2 \text{keV}) = 0.028 \pm 0.003$ . Fig. 3 shows soft versus hard  $\sigma_{rms}^2$  for Ton S 180 and the Seyfert 1 sample from N97a. Ton S 180 is one of several sources showing a greater  $\sigma_{rms}^2$  in the soft band than the hard.

#### 4. The Spectrum

While the difference in soft and hard variability properties means spectral variations are occurring, the hardness ratio is quite flat (Fig. 1) indicating that any spectral variability is of low amplitude and may be difficult to measure via spectral analysis. Consequently, we first discuss the mean spectrum from the observation.

We consider only the data in the 0.4 – 10 keV band. However, SIS data below 0.6 keV were excluded from the spectral analysis as it is commonly accepted that there are uncertainties associated with the *ASCA* calibration in that band. Whilst the SIS spectral calibration is suspect in this band, we do make use of the fact that the error is considered to be  $\lesssim 20\%$ , and that it causes the data to lay systematically low. Thus these data can sometimes be used to indicate which of several models may be most applicable. For example, if data in the 0.4-0.6 keV band lie above the extrapolation of our model, then

the source spectrum most likely does turn-up in the 0.4-0.6 keV range. Hence we take the approach of indicating where these data lie, although we never use them in a fit. This allows the reader to draw their own conclusions about the shape of the spectrum below 0.6 keV.

#### 4.1. Exclusion of the Fe K-shell regime

In this section we excluded the (rest-frame) 5.3-8.0 keV data, to temporarily remove the channels in which we expect to observe iron  $K\alpha$  emission in this source, so we could more easily parameterize the continuum shape.

Neither single nor double power-law models (attenuated by a column of neutral material) provided an acceptable fit due primarily to complexity in the  $\sim 0.6 - 1$  keV regime. The single power-law yielded  $\chi^2 = 953$  for 747 degrees of freedom (*dof*), the double power-law gave  $\chi^2/dof = 905/745$  Fig. 4a shows the ratio of the data to a power-law model with the 0.4-0.6 keV SIS data overlaid in dotted typeface.

The column density of the neutral absorber was consistent with the Galactic line-of-sight value ( $N_H = 1.52 \times 10^{20} \text{cm}^{-2}$ ; Stark et al. 1992) in the aforementioned fits and hence was fixed at that value subsequently. As shown in Fig. 4a the largest deviation is suggestive of an emission feature peaking just below 1 keV. An adequate fit is achieved when a broad gaussian emission line is added to the model. This gives an emission line rest-energy  $E = 0.82^{+0.20}_{-0.35} \text{keV}$ ,  $\sigma = 0.25^{+0.17}_{-0.03} \text{keV}$  and line flux of  $1.27 \times 10^{-3} \text{photons cm}^{-2} \text{s}^{-1}$ , yielding  $\chi^2/dof = 768/744$ , an improvement of  $\Delta\chi^2 = 185$  compared to a fit without this component (all errors are 90% confidence for the relevant number of interesting parameters in each case). Fig. 4b shows the data/model ratio after the fit. The improvement is immediately obvious. When the gaussian component is introduced into the model the underlying continuum is  $\Gamma = 2.50^{+0.08}$ . We note that with such a model, we find no requirement for a second power-law within the 0.6 – 10 keV band, although there is a suggestion of a spectral softening below 0.6 keV (as expected on the basis of *ROSAT* and *BeppoSAX* results). The equivalent width (EW) of the line was  $155^{+262}_{-65} \text{eV}$ , and could represent the sum of contributions from species such as ionized Ne and Fe-L emission. To parameterize the emitting gas, we fit the data using the “mekal” model for emission from a thermal plasma, which is based on Mewe & Kaastra 1992, this includes important iron L calculations (Liedahl, Osterheld & Goldstein 1995) and we assumed cosmic abundances. This fit equated the soft emission to that expected from an optically thin plasma in collisional equilibrium with  $kT=0.84 \text{ keV}$ , although the overall fit gave  $\chi^2/dof = 798/745$  (a 9% probability of achieving this fit statistic by chance); inferior to that provided using a simple gaussian parameterization. The inferiority of the mekal model could be due to the

assumption of cosmic abundances which leads to the prediction of observable O, Si and S lines from the gas, or may indicate the emission is from photoionized gas. These data do not allow us to distinguish between these possibilities.

Alternatively, the soft line could represent a single, relativistically-broadened line. We fit it using the disk-line model profile of Fabian et al. (1989). That model assumes a Schwarzschild geometry and computes the line profile.

We assumed the line originates from a disk between radii,  $r$ , from 6 to 1000  $r_g$ , where the gravitational radius,  $r_g = GM/c^2$  for a black hole of mass  $M$ . The line emissivity function was assumed to be  $r^{-2.5}$ , typical of Seyfert 1 galaxies (N97a). The inclination of the disk relative to the observer is defined such that  $i = 0$  is a face-on disk. The fit was inferior to the gaussian model ( $\chi^2/dof = 786/744$ ) yielding a rest-energy  $E = 0.86^{+0.30}_{-0.30}$  keV, an inclination  $i > 77^\circ$ ,  $\Gamma = 2.58^{+0.08}_{-0.08}$  with equivalent width  $EW = 88^{+130}_{-33}$  eV. The poor constraints on energy do not allow us to unambiguously identify the line, although we note that OVIII, NeIX, NeX and emission from the Fe L-shell are expected to provide strong emission at energies consistent with the fitted value.

We also considered alternative models based upon the possibility that the observed shape of the soft X-ray spectrum is due to the presence of several strong absorption edges. First we fit the data to a power-law plus two absorption edges. This yielded a rest-energy  $E_1 = 0.51^{+0.16}_{-0.01p}$  keV, where  $p$  indicates an error range reached the maximum or minimum allowed value for the parameter. The optical depth of this edge was  $\tau_1 = 0.44^{+25}_{-0.35}$ . The second edge could be characterized with a rest-energy  $E_2 = 1.42^{+0.05}_{-0.06}$  keV,  $\tau_2 = 0.25^{+0.05}_{-0.06}$  and the fit gave  $\chi^2/dof = 841/743$ . This was clearly less satisfactory than the gaussian emission model (Fig. 4c). However, a detailed consideration of this model is interesting as three Seyferts with similar characteristics to Ton S 180 have shown deep absorption features close to 1 keV. Leighly et al. (1997) interpreted those as evidence for absorption in outflowing material with velocities in the range 0.2-0.6c. In Ton S 180, the lower energy edge is consistent with neutral oxygen. However, while there are several edges that could be identified with the feature at 1.42 keV, none of them would be expected to arise from neutral material. Thus we consider whether the two edges might both arise from ionized material, flowing into or out from the nucleus. However, fits to a warm absorber found no satisfactory solution, even when the ionization-state and redshift of the absorber were totally unconstrained such that relativistic velocities were allowed as possible solutions. The failure to find a satisfactory fit, even allowing a strong blueshift for the absorber, leads us to conclude that if the features are due to absorption edges, then they are not consistent with both arising in a single zone of outflowing material.

We also tried a broken power-law model for the continuum with a single absorption

edge (c.f. Fig. 4a). This model provides an adequate description of the data, yielding a fit-statistic  $\chi^2/dof = 770/743$ . The fit gave  $\Gamma_{soft} = 3.66_{-0.27}^{+0.28}$  meeting  $\Gamma_{hard} = 2.56_{-0.08}^{+0.07}$  at a break point of  $1.50_{-0.08}^{+0.09}$  keV with an edge of depth  $\tau \sim 1.50_{-0.48}^{+0.32}$  at  $E = 0.61_{-0.02}^{+0.02}$  keV. However, when this model is extrapolated down to 0.4 keV, and compared to the SIS data, there is clearly a huge discrepancy. Fig. 4d) shows the data/model ratio, which indicates that the extrapolation of this model down to 0.4 keV overpredicts the flux by a factor of  $\sim 3$  compared to the data. This mis-match far exceeds any *ASCA* calibration uncertainty and indicates that this is an unsatisfactory model (c.f. Orr et al. 1998).

Fink et al. (1997) also noted similar spectral complexity in PSPC spectra of Ton S 180, although their interpretation was different, based upon the limited spectral range available using the PSPC. Their favored model was an absorbed power-law, plus a black body of temperature  $kT \sim 16$  eV, dominating below 0.3 keV. The latter would not be visible in the *ASCA* band but in any case the *ROSAT* model of Fink et al. (1997) is inconsistent with our *ASCA* data. Specifically, their power-law component is too steep to be consistent with our hard X-ray data. However, the evidence for spectral features looks similar in both instruments, so it is interesting to examine some of the PSPC data in light of the *ASCA* result. We selected the 1993 June 16 data, which was the last and longest observation of Ton S 180 by the PSPC. This revealed a photon index  $\Gamma = 2.96_{-0.03}^{+0.03}$  with no intrinsic absorption over the Galactic line-of-sight value. The data/model ratio confirms the spectral complexity (Fig. 5), as noted by Fink et al. (1997). Those authors modeled the shape we see as a juxtaposition of two continuum components, but we favor an emission feature. Our power-law plus gaussian model from the *ASCA* data is consistent with the PSPC data. The strength of the gaussian component cannot be usefully constrained fitting the latter but is consistent with the *ASCA* result. Thus, these PSPC data increase our confidence as to the reality of the feature seen in the SIS data. The PSPC data also indicate the presence of additional spectral features, perhaps deep absorption close to 0.4 keV. Although the PSPC has proved a reliable “finder” for interesting sources, it does not allow us to unambiguously determine the origin of the spectral complexity. We cannot distinguish between our solution and the model favored by Fink et al. (1997), thus we do not attempt to model the PSPC data in more detail.

No soft X-ray feature was detected in the *BeppoSAX* observation (Comastri et al. 1998), but the exposure in the LECS was very low. Also, the LECS has a slightly lower energy resolution,  $FWHM \sim 200$  eV at 1 keV compared to  $FWHM \sim 110$  eV at 1 keV for the *ASCA* SIS, during the Ton S 180 observation. The *BeppoSAX* model is also inconsistent with the *ASCA* data, primarily because the former lacks any parameterization of the soft spectral hump. As noted by Fink et al. (1997), the source exhibits spectral variations, so we should not expect perfect consistency between the *ROSAT*, *BeppoSAX* and *ASCA* data.

In an attempt to gain further insight, we examined the extrapolation of various models and compared them to infrared data; optical data; ultraviolet data from both the International Ultraviolet Explorer (*IUE*) plus *EUVE* and PSPC data (Fig. 6). All the fluxes were absorption-corrected and taken from Vennes et al. (1995). It is obvious that the broken power-law model provides the least satisfactory extrapolation to lower energies. The steep part of the broken power-law is  $\Gamma \sim 3.7$ . It can be seen that for Ton S 180 such a steep component overpredicts the *EUVE* flux by an order of magnitude. If the soft X-ray continua are this steep, then there is a flattening of the spectrum within the *ROSAT* PSPC bandpass. However, we reject this solution, based upon the large discrepancy of this model compared to the 0.4–0.6 keV *ASCA* data. The continua from the other two models are consistent with a simple extrapolation down to the *IUE* bandpass, within a factor consistent with the source variability amplitude, and do not require any additional component peaking in the (unobserved) XUV regime (between  $\sim 0.01$  and 0.1 keV). In these cases the model has to turn over close to the *IUE* bandpass, in order to explain the infrared and optical data. We return to these points in the discussion.

#### 4.2. The Iron $K\alpha$ Line

Analysis of the iron  $K\alpha$  line is particularly interesting in the light of the *BeppoSAX* result. Comastri et al. (1998) found evidence for line emission at  $\sim 7$  keV, indicative of an origin from material containing ionized iron, consistent with the iron recombination line from H-like iron at 6.94 keV. So, having found an adequate parameterization of the continuum shape, we returned the 5.3 – 8.0 keV (rest-frame) data to the analysis, and examined the data/model ratio (versus the best-fit continuum model). Fig. 7 shows this ratio, which indicates the presence of significant line emission attributable to iron  $K\alpha$ , apparently peaking close to  $\sim 7$  keV in the rest-frame, confirming the *BeppoSAX* result. We fit the line with a redshifted, narrow gaussian component which yielded a reduction in  $\chi^2$  by 18, giving  $\chi^2/dof = 882/851$ , compared to a model without the component. The rest-energy was  $E = 6.92_{-0.23}^{+0.23}$  keV for a line of equivalent width  $EW = 316_{-201}^{+198}$  eV. However, the line profile appears broad, and allowing the width of the model line to be free achieved a further reduction in  $\chi^2$  by 5, significant at  $> 95\%$  confidence. That fit yielded a rest-energy  $E = 6.44_{-0.44p}^{+1.06}$  keV, where  $p$  indicates the error search hit the limit allowed for the parameter. The line width was large  $\sigma = 1.0_{-0.88}^{+0p}$  keV, and  $EW = 963_{-692}^{+361}$  eV. Such a large width, and discrepancy between the best-fit energy using narrow versus broad-line models indicates the asymmetry of the line is significant. Thus we attempted some further models. We replaced the broad gaussian with two narrow gaussian lines. One had the line energy fixed at a rest-energy 6.4 keV, the other had the energy free. This fit gave no



statistical improvement over the broad-line model, and had two more degrees of freedom. It yielded a rest-energy  $E = 7.01_{-0.21}^{+0.24}$  keV, and  $EW = 333_{-210}^{+204}$  eV plus an equivalent width for the 6.4 keV line of  $EW = 150_{-150}^{+156}$  eV. This indicates that emission from highly ionized material provides a significant contribution to the overall iron  $K\alpha$  flux, which is also evident from inspection of Fig. 7.

The asymmetry of the profile prompted us to fit the iron  $K\alpha$  line using the disk-line model profile as described in §4.1. This fit gave  $i = 39^{\circ}_{-39}^{+21}$ ,  $E = 6.61_{-0.21}^{+0.25}$  keV (rest-energy) and  $EW = 814_{-869}^{+438}$  eV, with a fit-statistic similar to that obtained with the broad gaussian parameterization, with the same number of degrees of freedom. We note that the inclination implied from fitting the soft line with this model is inconsistent with the inclination inferred from fitting the iron K-shell line. The most likely possibility seems to be that the soft X-ray feature is not dominated by a single species originating in an accretion disk.

## 5. Spectral Variability

Ton S 180 shows a significantly greater  $\sigma_{rms}^2$  in the soft band compared to the hard band, as described earlier. This indicates the spectrum of the source is variable, so we selected spectra from high and low states for comparison. First we split the data using an intensity division equivalent to an SIS0 count rate of 0.65 ct/s which yielded high-state and low-state spectra with a similar number of counts in each. However, no significant difference was seen in any parameter when using this intensity selection. Next we isolated data taken during the peaks of the two flares, as indicated on Fig. 1, and compared those spectra with the remainder of the data. This yielded “flare” and “quiescent” spectra with 0.5–2 keV fluxes  $1.40 \times 10^{-11}$  erg cm<sup>-2</sup>s<sup>-1</sup> and  $1.08 \times 10^{-11}$  erg cm<sup>-2</sup>s<sup>-1</sup>, respectively, and 2–10 keV fluxes  $6.96 \times 10^{-11}$  erg cm<sup>-2</sup>s<sup>-1</sup> and  $5.85 \times 10^{-12}$  erg cm<sup>-2</sup>s<sup>-1</sup>, respectively. Thus the “flare” state is 20% higher than the “quiescent” state in the 2 – 10 keV band, and 30% higher in the 0.5 – 2 keV band.

No significant variability was seen in the soft-bump. However, the spectral slope appeared slightly steeper and the Fe  $K\alpha$  line stronger during the flares. These two parameters are very highly correlated in these fits. To determine which component was most likely variable we calculated the 90% confidence contours for photon index versus line intensity for the Fe  $K\alpha$  line (Fig. 8). These contours suggest that the line is more intense during the flare state, while the suggested steepening of the photon index appears less significant. We also find that the equivalent width of the line appears to *increase* with flux. The equivalent width during the high-state lies above the 90% confidence range determined for the low-state; we find  $EW_{low} = 421_{-328}^{+700}$  eV and  $EW_{high} = 1630_{-1078}^{+760}$  eV.

Thus, while there appears to be a global X-ray Baldwin effect observed across samples of QSOs, whereby the equivalent width of the iron  $K\alpha$  line is seen to reduce with increasing luminosity (Iwasawa & Taniguchi 1993), this does not appear to be true for luminosity variations in this object and in fact the opposite behaviour is observed. An increase in  $EW$  with increased flux indicates a significant change in the conditions of the reprocessor with changing flux. One possible explanation is rapid changes in the fluorescent yield of the reflector, giving more line photons in the high-state because the material is more highly ionized. If true, this would be accompanied by a shift of the line peak to higher energies as the source flux increases. Unfortunately we cannot determine whether such an energy shift occurs, using these data. These results on changes in the iron  $K\alpha$  line should be considered tentative, as the fit parameters indicate there are only  $\sim 200$  photons in the line during the times selected for the flares, and  $\sim 350$  during the remainder of the observation.

## 6. Summary of Observational Results

We present an *ASCA* observation of Ton S 180 which shows:

- Factor-of-two variability in X-ray flux over a few thousand seconds, with significantly higher  $\sigma_{rms}^2$  in the 0.5–2 keV band, than in the 2–10 keV band. This source also shows much higher  $\sigma_{rms}^2$  than other Seyfert galaxies, predominantly due to the greater degree of variability in the soft band.
- A power-law with photon index  $\Gamma \sim 2.5$  provides an adequate parameterization of the continuum across 0.6–10 keV with no intrinsic X-ray absorption
- A complex soft X-ray spectrum which can be parameterized as a blend of line emission peaking in the 0.7-1.0 keV regime
- A confirmation of Fe K-shell emission from highly-ionized Fe in this source. Furthermore, the *ASCA* data show the line profile to be broad and asymmetric
- A tentative suggestion of rapid variability in the iron K-shell line, with an increase in line flux and equivalent width during X-ray flares.

## 7. Discussion

Ton S 180 shows larger amplitude variations than Seyfert 1 galaxies of comparable luminosity, when sampled on a timescale of 128 s. Variations of large amplitude could

indicate that we are seeing X-rays from a more compact region in NLSy1 galaxies, and if we assume these X-rays originate in the accretion disk then either the disk is more compact or perhaps extends closer to the black hole. The latter would be possible if the hole has a greater degree of rotation in NLSy1 galaxies than in Seyfert 1 galaxies, as suggested by authors such as Forster & Halpern (1996). Another simple possibility is that in NLSy1s the bulk of the X-ray emission is seen directly, or with fewer scatterings than the emission observed from Seyfert 1 galaxies of the same luminosity. This could be a result of a physical difference in the scattering region in NLSy1 versus other Seyfert galaxies, or could be a result of differences in the orientation for the two types of Seyfert such that light paths to the observer are different. Instabilities can occur in the inner accretion disk when the accretion rate is greater than a small fraction of maximum rate allowed by the Eddington limit (e.g. Shakura & Sunyaev 1976), and these could manifest themselves as variations in X-ray flux. So, another interesting possibility is that the differences in spectral and variability properties between NLSy1 and Seyfert 1 galaxies both originate as a result of a higher accretion rate in NLSy1s.

Ton S 180 also shows higher variability ( $\sigma_{rms}^2$ ) in the soft band, than the hard. This behavior is like that observed in NGC 4051, Mkn 766, NGC 3227 and NGC 3516 (N97a). In NGC 3227 this is attributed to changes in the emission components rather than the absorber (George et al. 1998b). In NGC 3516 we know that  $FWHM\ H\beta \sim 6800$  km/s (Osterbrock 1977), and the observation of this behaviour in NGC 3516 indicates the phenomenon is not restricted to Seyferts with narrow  $H\beta$ . For Ton S 180, the absence of any significant intrinsic X-ray absorption means that the stronger variations in the soft versus hard flux are unlikely to be attributable to variable opacity in an absorber. This in turn indicates that the difference is likely to be due to changes in the continuum slope or the relative strength of emission components, as inferred for NGC 3227 (George et al. 1998b). A *possible* interpretation is that the photons at higher X-ray energies are produced by upscattering of soft photons, the scattering process could dilute the observed variability by an amount dependent of the size of the scattering region. Alternatively there may be more or larger perturbations in the region where the soft photons are produced. We were unable to satisfactorily quantify the spectral variability through flux-divided spectral analysis.

The mean spectrum reveals a photon index  $\Gamma \sim 2.5$  extending to 10 keV. This supports the conclusion by Brandt et al. (1997) that sources with narrow permitted lines have steeper continua in the 2 – 10 keV band than those with broad permitted lines. Furthermore, Ton S 180 is consistent with the distribution for  $\Gamma$  versus  $H\beta$ , shown in Brandt et al. (1997).

We find strong evidence for a complex soft X-ray spectrum, confirming indications from PSPC data (Fink et al. 1997). Ton S 180 shows a hump of X-ray emission peaking at

a rest-energy close to 0.9 keV. This could be due to a blend of line emission, predominantly from ionized species of Ne and from the Fe L-shell. The observed feature is broadly consistent with thermal emission from a plasma of temperature  $\sim 0.84$  keV. The soft X-ray spectrum is also qualitatively similar to that predicted when nuclear radiation is reprocessed in small, dense clouds that are optically thin to Thomson scattering (Kuncic et al. 1997). Somewhat similar spectral complexity is also observed in quasars (Nandra et al. 1998), indicating this may be a common phenomenon and an important component of the X-ray spectrum. The observed hump could be the peak of emission from a hot continuum component, however, contrary to Nandra et al. 1998) we find a blackbody component to be too broad to satisfactorily explain the observed feature in this source.

The emission from an ionized accretion disk yields a spectrum rich in emission lines (e.g. Zycki et al. 1994; Ross & Fabian 1993; Matt, Fabian & Ross 1993) for some accretion rates. This means that the presence of emission lines can be an important indicator of the accretion rate in a source, although unfortunately we cannot usefully constrain that quantity using these data, and with current models. For high accretion rates, the disk becomes highly ionized. An ionized disk has a reduced cross-section at low energies, so the contrast between the continuum and reflected emission will be greatly reduced. In the case of Ton S 180 the continuum is very steep, giving rise to relatively few photons above  $\sim 10$  keV from which to produce a Compton Reflection hump. The absence of a hard spectral component, and the profile of the iron K-shell line are consistent with the picture of an ionized disk in this source.

We confirm the discovery by Comastri et al. (1998) of iron K-shell emission peaking close to 7 keV. Furthermore, these *ASCA* data show the iron K-shell line to be broad and asymmetric. The shape of the line profile suggests an origin in an accretion disk, rather than a blend of unresolved narrow lines from regions further out. While the individual parameters are poorly constrained in the diskline fit, the line is clearly significantly different to the mean profile obtained for Seyfert 1 galaxies, which could be due to either a difference in ionization or orientation of the reprocessor. We favor higher ionization of the disk as an explanation for two reasons. First, the high equivalent width of the line is difficult to explain if the disk is edge-on, as absorption of the line photons is expected within the disk (e.g. George & Fabian 1991). Second, the soft X-ray spectrum supports the existence of an ionized reprocessor in this source. Whilst we did not find a good fit to the soft X-ray feature using a single diskline in §4.1, as stated above, ionized disk models can predict emission from several highly-ionized species in the  $\sim 0.7$ – $1.5$  keV band. It is therefore possible that the soft emission feature is a blend of such lines; unfortunately the quality of the *ASCA* data is insufficient to allow the deconvolution of such a blend.

This result is particularly intriguing in the light of the apparent correlation between the profile of the Fe K-shell line and 2–10 keV luminosity, for a sample of quasars (Nandra et al. 1997b). Those authors find that the red wing and 6.4 keV peak of the line decrease with increasing nuclear luminosity, which is an extension of the X-ray Baldwin effect. The 2 – 10 keV luminosity of Ton S 180 is  $\sim 10^{44}$  erg s<sup>-1</sup> putting Ton S 180 on the borderline where line profile changes start to be seen in the quasar sample (Nandra et al. 1997b). Of course some distribution is expected on a source-by-source basis, if not in the intrinsic relationship then certainly in the observed relationship, since there could be some difference in the luminosity which is observed and that which is incident on the reprocessor.

Time-resolved spectroscopy tentatively suggests the strength of the iron K $\alpha$  line increases when the continuum flares occur. If confirmed, the rapid response of the line would strongly confirm its proposed origin in an ionized disk, the bulk of the line arising within a few light hours of the active nucleus. As noted by Comastri et al. (1998), relativistic boosting would be expected to affect the iron K-shell line if it is produced very close to the black hole, thus the correlation of line and continuum would suggest the flare events are due to perturbations close to the central black hole, while the longer timescale variations are fundamentally different in nature and are not necessarily accompanied by changes in the line strength.

The complexity of the spectrum and the cutoff of the (reliable) *ASCA* data at 0.6 keV leave us insensitive to any continuum softening, and we do not require a steepening of the power-law continuum within the 0.6 – 10 keV band. Laor et al. (1997) dispute the existence of a large bump peaking in the XUV, based upon *ROSAT* observations of quasars. As demonstrated in Fig. 6, our preferred solution is consistent with a simple extrapolation of the *ASCA* continuum down to the *IUE* bandpass, in agreement with the Laor result (allowing that the *EUVE* point is high by a factor which is consistent with the source amplitude of variability). Korista, Ferland and Baldwin (1997) have discussed the general problem that extrapolating the known soft X-ray spectrum of AGN down to the *EUVE* and *IUE* bands there appear to be too few 54.4 eV photons to account for the strength of observed HeII lines. They consider the possibility that the broad-line clouds see a different continuum than the observer does, or that the XUV spectrum has a double-peaked shape. *AXAF* and *XMM* observations of this source are clearly required, to unambiguously resolve the X-ray emission lines and thus to allow us to tightly constrain the X-ray continuum in order to determine whether this component really does extrapolate to meet the UV data.

## 8. Acknowledgements

We are grateful to *ASCA* team for their operation of the satellite and to the referee, Smita Mathur, for comments which significantly improved the paper. This research has made use of the NASA/IPAC Extragalactic database, which is operated by the Jet Propulsion Laboratory, Caltech, under contract with NASA; of the Simbad database, operated at CDS, Strasbourg, France; and data obtained through the HEASARC on-line service, provided by NASA/GSFC. We acknowledge the financial support of Universities Space Research Association (IMG, TJT) and the National Research Council (KN).

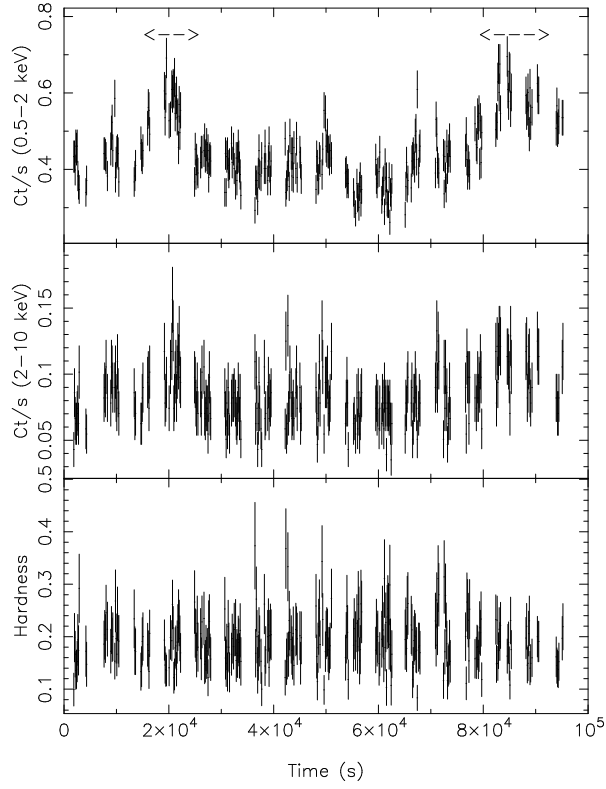


Fig. 1.— The light curves in 128 s bins for the combined SIS data in the 0.5-2 keV band (top panel) and 2-10 keV band (middle panel). The ratio of 2-10 keV/0.5-2 keV counts is shown in the panel. The arrows indicate the periods of data taken to be the “flare-states”, as discussed in §5.

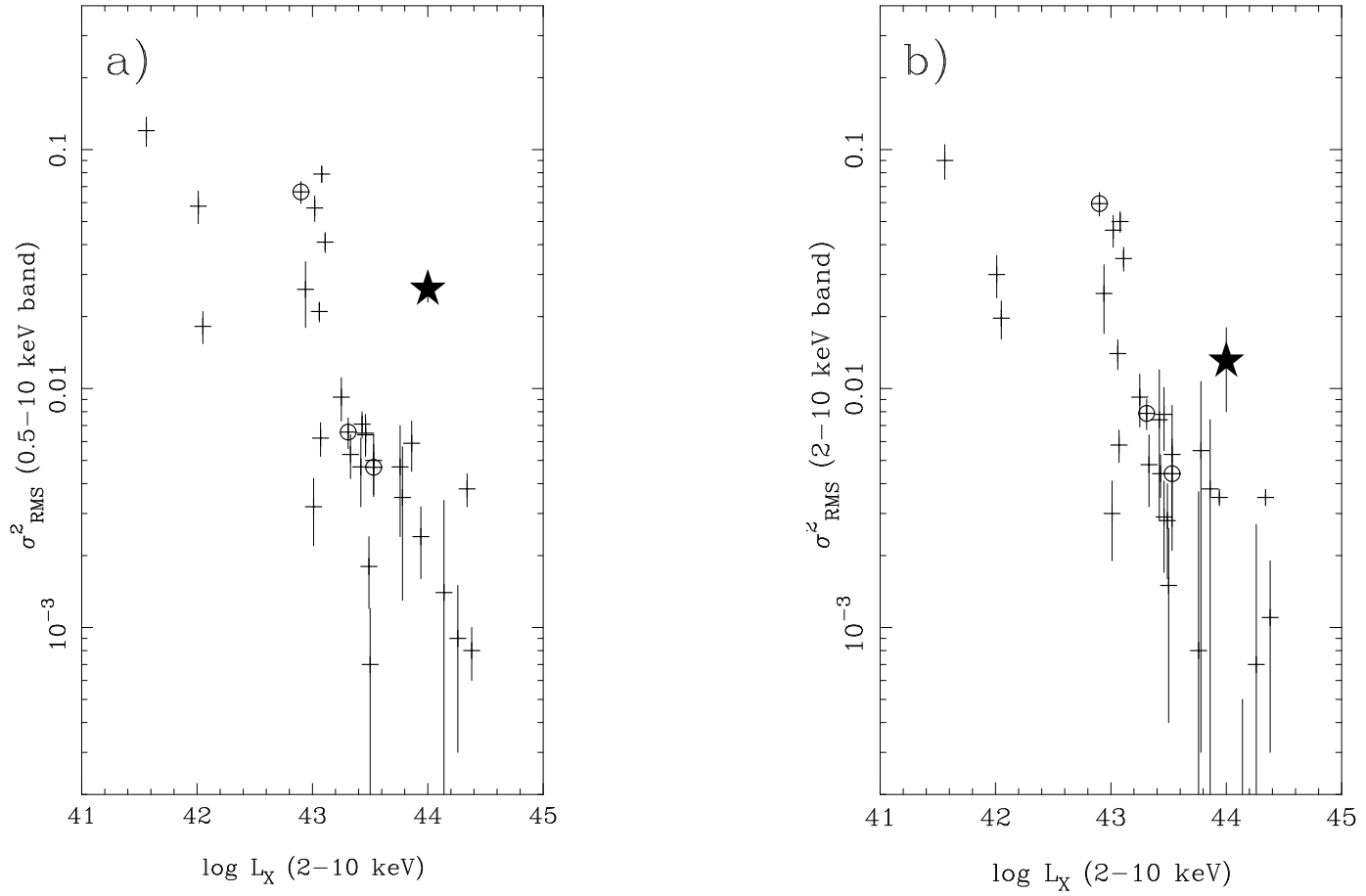


Fig. 2.— a) Normalized excess variance ( $\sigma_{rms}^2$ ), taken over the 0.5-10 keV band, versus luminosity for the Seyfert 1 sample from N97a; George et al. 1998a,b (crosses); a few Seyfert type 2 galaxies from Turner et al. 1997 (crossed circles) and Ton S 180 (star) which lies significantly above the rest of the distribution; b) in this plot  $\sigma_{rms}^2$  is taken over the 2-10 keV band and Ton S 180 lies close to the rest of the distribution.



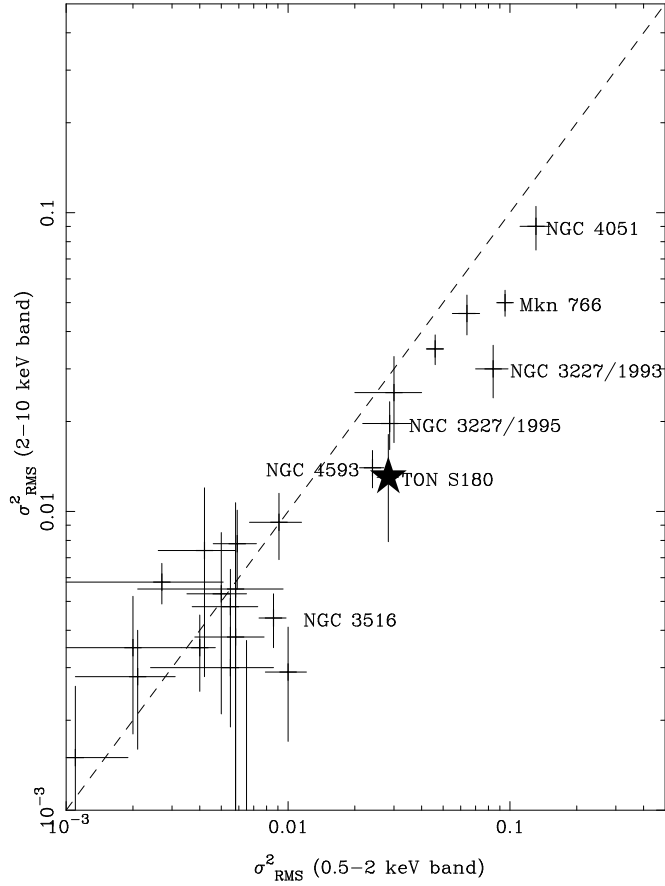


Fig. 3.— The excess variance  $\sigma_{rms}^2$  in the soft band, 0.5-2 keV, versus that in the hard band, 2-10 keV, for the SIS data. The Seyfert 1 sample (N97a; George et al. 1998a,b) are shown as crosses. Ton S 180 is shown as a star, and has a higher  $\sigma_{rms}^2$  in the soft band than in the hard, as discussed in the text.

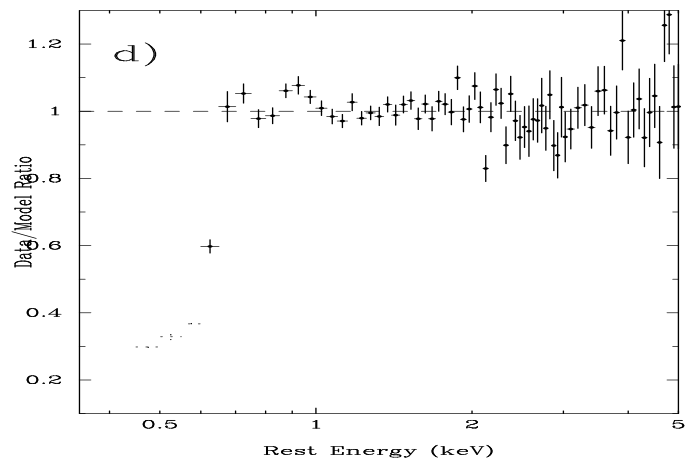
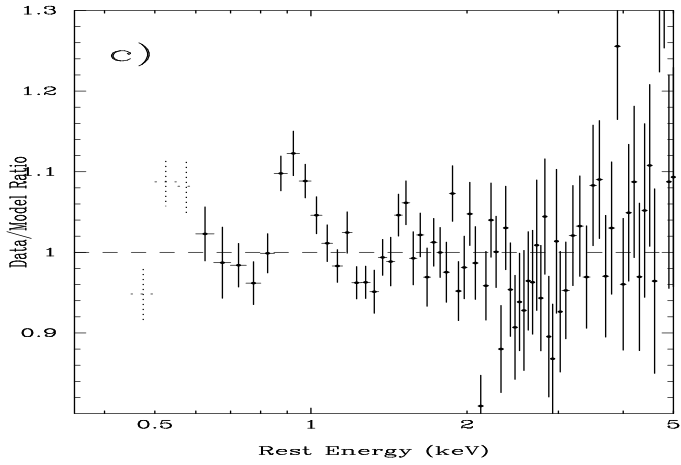
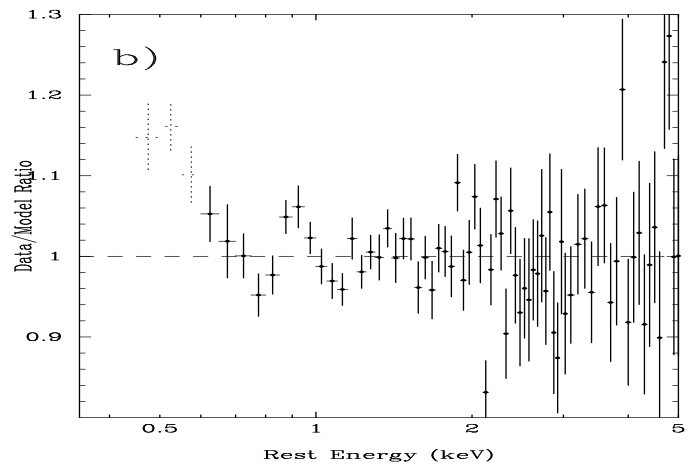
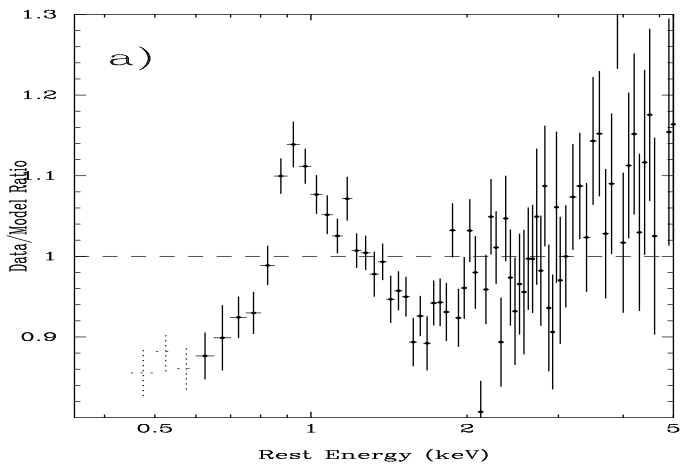


Fig. 4.— a) The data/model ratio from the combined SIS+GIS data, compared to a power-law model. The dotted points show the SIS data from the 0.4-0.6 keV band, which were not used in the fit but have been overlaid for illustrative purposes; b) data are compared to power-law model with broad gaussian emission line; c) data are compared to a power-law plus two absorption edges; d) data are compared to a broken power-law model with a single edge, showing the large discrepancy between this model and the low energy data.

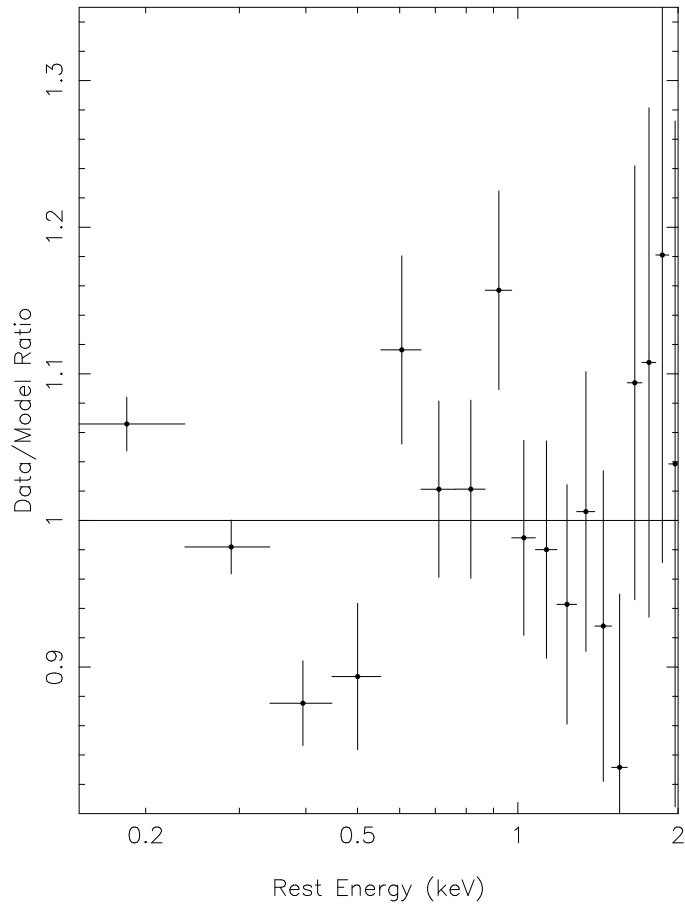


Fig. 5.— The data/model ratio compared to a power-law model, for the *ROSAT* PSPC data.

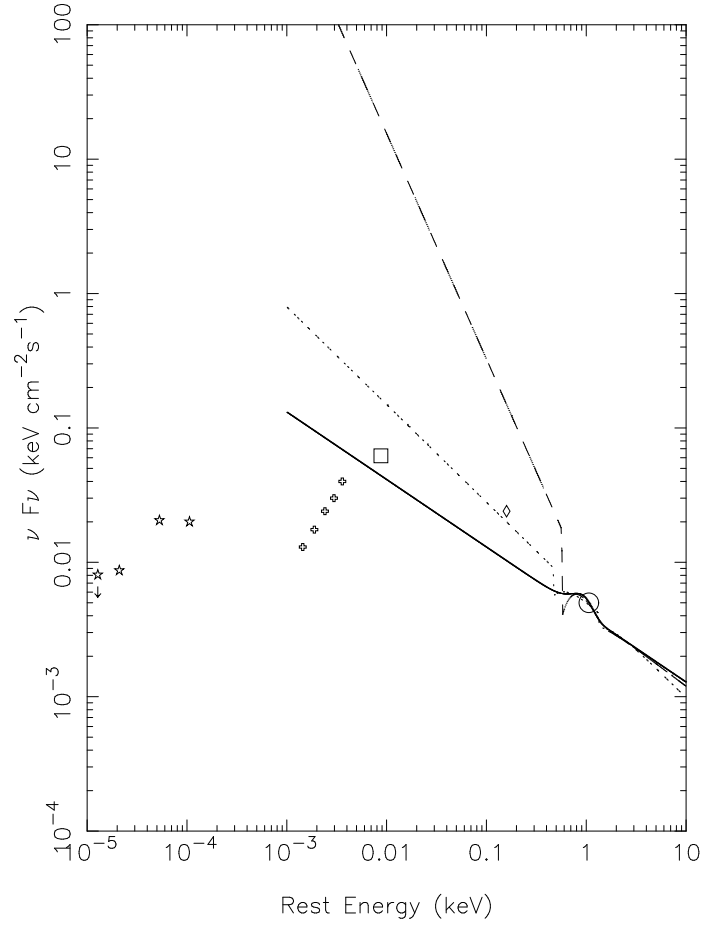


Fig. 6.— Three models for the *ASCA* data, compared to the absorption-corrected infrared data (open stars), the optical U,V,B,R,I fluxes (open crosses), *IUE* data (open box), *EUVE* data (open diamond) and the *ROSAT* PSPC data (open circle). The dashed model line represents the broken power-law with single edge; the dotted line represents the single power-law with two edges; the solid line represents the single power-law plus emission feature.

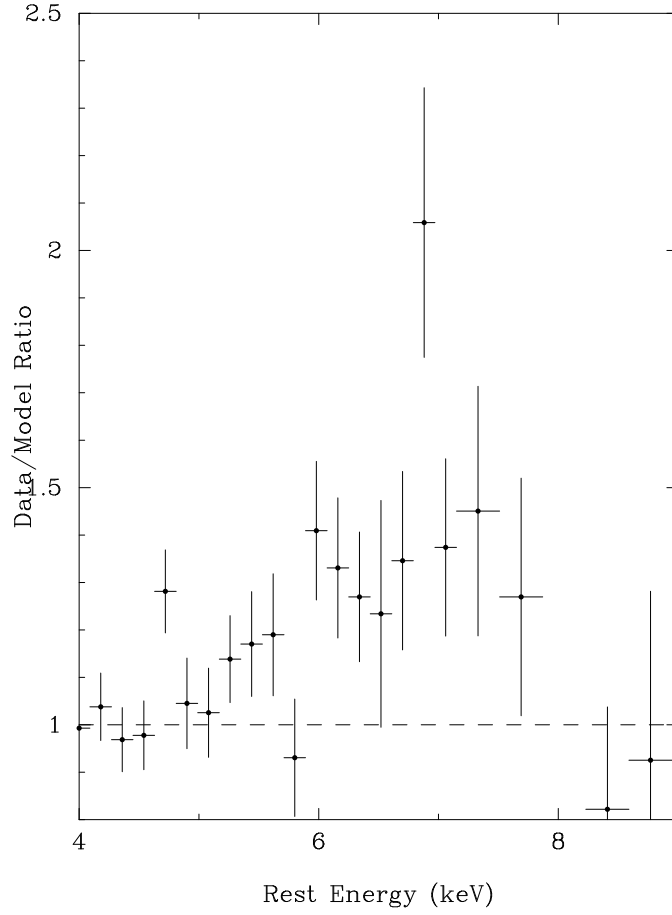


Fig. 7.— Data/model ratio based on the combined SIS+GIS data, transformed into the rest-frame. The continuum was fit without the (rest-frame) 5.3 – 8 keV data, using the power-law model with the soft hump fit by a broad gaussian (as described in the text). The 5.3 - 8.0 keV data were then overlaid and have been rebinned for clarity. These data indicate line flux distributed asymmetrically across the 5.0 - 8.0 keV range with a peak close to a rest-frame energy of 7 keV.

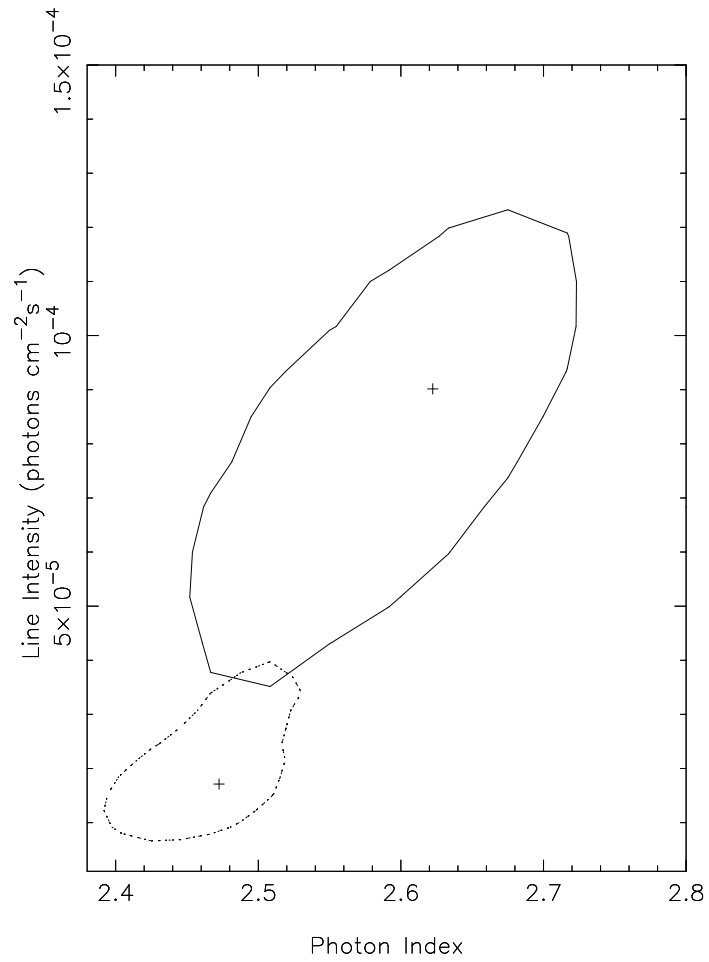


Fig. 8.— Contours indicating the 90% confidence limit for photon index versus intensity of the iron K-shell line. The solid line represents the flare-state while the dotted line represents the remainder of the observation. The best-fitting values are indicated by crosses.

## REFERENCES

- Boller, T., Brandt, W.N., Fink, H.H., 1996, A&A, 305, 53
- Brandt, W.N., Mather, S., Elvis, M., 1997, MNRAS, 285, L25
- Bowyer, S. et al. 1996, A&A, 305, 53
- Burke, B.E., Mountain, R.W., Daniels, P.J., Dolat, V.S., 1994, IEEE Trans. Nuc. SCI. 41, 375
- Comastri, A. et al. 1998, A&A, in press
- Fabian, A.C., Rees, M.J., Stella, L., White, N.E. 1989, MNRAS 238, 729
- Fink, H.H., Walter, R., Schartel, N., Engels, D., 1997, A&A, 317, 25
- Forster, K., Halpern, J., 1996, ApJ, 468, 565
- George, I.M., Mushotzky, R.F., Turner, T.J., Yaqoob, Y., Ptak, A., Nandra, K., Netzer, H., 1998b, ApJ, submitted
- George, I.M., Mushotzky, R.F., Turner, T.J., Netzer, H. Nandra, K., 1998a, ApJ, in press
- Halpern, J.P. & Oke, J.B., 1987, ApJ, 312, 91
- Hwang, C-Y., Bowyer, S., 1997, ApJ, 475, 552
- Iwasawa, K. & Taniguchi, Y., 1993, ApJ, 413, 15
- Korista, K., Ferland, G. & Baldwin, J., 1997, ApJ 487, 555
- Kuncic, Z., Celotti, A., Rees, M., 1997, MNRAS, 284, 717
- Laor, A., Fiore, F., Elvis, M., Wilkes, B.J., McDowell, J.C., 1997, ApJ 477, 93
- Lawrence, A., Elvis, M., Wilkes, B.J., McHardy, I., Brandt, W.N., 1997, MNRAS, 285, 879
- Liedahl, D.A., Osterheld, A.L., Goldstein, W.H., 1995, ApJ, 438, L115
- Leighly, K., Mushotzky, R., Nandra, K., Forster, K., 1997, ApJ, 489, L25
- Makishima, et al 1996, PASJ, 48, 171
- Matt, G., Fabian, A.C., Ross, R.R., 1993, MNRAS 264, 839
- Mewe, R., & Kaastra, J.S., 1992, "An X-ray Spectral Code for Optically Thin Plasmas", an internal SRON-Leiden Report, v 2.0)
- Nandra, K., George, I.M., Mushotzky, R.F., Turner, T.J., Yaqoob, T., 1997, ApJ, 476, 70 (N97a)
- Nandra, K., George, I.M., Mushotzky, R.F., Turner, T.J., Yaqoob, T., 1997, ApJ 488, L91 (N97b)

Nandra, K., George, I.M., Mushotzky, R.F., Turner, T.J., Yaqoob, T., 1998, in prep  
Ohashi, T., et al., 1996, PASJ, 48, 157  
Orr, A., Yaqoob, T., Parmar, A.N., Piro, L., White, N.E., Grandi, P., 1998, A&A,  
submitted.  
Osterbrock, D.E., 1977, ApJ 215, 733  
Pounds, K.A., Done, C., Osborne, J.P., 1995, MNRAS, 277, L5  
Ross, R.R., Fabian, A.C. 1993, MNRAS 261, 74  
Shakura, N.I., Sunyaev, R.A., 1976, MNRAS, 175, 613  
Stark, A.A., Gammie, C.F., Wilson, R.W., Bally, J., Linke, R.A., Heiles, C., Hurwitz, M.,  
1992, ApJS, 79, 77  
Turner, T.J., George, I.M., Nandra, K. & Mushotzky, R.M., 1997, ApJ in press  
Vennes, S., Polomski, E., Bowyer, S., Thorstensen, J.R., 1995, ApJ, 448, L9  
Wisotzki, A., Dreizler, S., Engels, D., Fink, H.H., Heber, U., 1995, A&A, 297, L55  
Zycki, P.T., Krolik, J.H., Zdziarski, A.A., Kallman, T.R., 1994, ApJ, 437, 597